

## MicroRNA-21 Modulates the Levels of Reactive Oxygen Species by Targeting SOD3 and TNF $\alpha$

Xiangming Zhang<sup>1</sup>, Wooi-Loon Ng<sup>1</sup>, Ping Wang<sup>1</sup>, LinLin Tian<sup>1</sup>, Erica Werner<sup>2</sup>, Huichen Wang<sup>1</sup>, Paul Doetsch<sup>1,2</sup>, and Ya Wang<sup>1</sup>

### Abstract

MicroRNA-21 (miR-21) is an oncomir overexpressed in most human tumors in that it promotes malignant growth and progression by acting on multiple targets. Here, we broaden the impact of miR-21 in cancer by showing that it regulates the formation of reactive oxygen species (ROS) that promote tumorigenesis. Key targets of miR-21 in mediating this function were SOD3 and TNF $\alpha$ . We found that miR-21 inhibited the metabolism of superoxide to hydrogen peroxide, produced either by endogenous basal activities or exposure to ionizing radiation (IR), by directing attenuating SOD3 or by an indirect mechanism that limited TNF $\alpha$  production, thereby reducing SOD2 levels. Importantly, both effects contributed to an elevation of IR-induced cell transformation. Our findings, therefore, establish that miR-21 promotes tumorigenesis to a large extent through its regulation of cellular ROS levels. *Cancer Res*; 72(18); 4707–13. ©2012 AACR.

### Introduction

MicroRNAs (miR) are a class of small noncoding RNAs comprising approximately 22 nucleotides in length. In general, miRs negatively regulate gene expression posttranscriptionally by binding to the 3'-untranslated region (UTR) of the targeted mRNA to inhibit gene translation. One miR is capable of targeting multiple mRNAs and one mRNA can be targeted by multiple miRs. Most mammalian mRNAs are conserved targets of miRs. Among more than 1,400 miRs that have been documented, miR-21 is overexpressed in multiple human cancers (1) and miR-21 upregulation induced tumorigenesis in a mouse model (2, 3) and in human cells (4), indicating a central role of miR-21 in carcinogenesis. Although, multiple targets of miR-21 have been identified, including tumor suppressors *PTEN*, *PDCD4*, and *TPMI* (5–9), the whole picture for miR-21-induced tumorigenesis remains unclear.

Reactive oxygen species (ROS) generated from endogenous metabolic processes or exogenous ionizing radiation (IR) exposure, are mutagenic, and it is widely accepted that ROS promotes tumorigenesis (10, 11). Superoxide (O<sub>2</sub><sup>•-</sup>) and hydrogen peroxide (H<sub>2</sub>O<sub>2</sub>) are the major ROS species. The human superoxide dismutase (SOD) family includes 3 members SOD1, SOD2, and SOD3 and are the major enzymes metabolizing ROS by converting superoxide to hydrogen peroxide [M<sup>(n+1)+</sup> – SOD +

2O<sub>2</sub><sup>-</sup> + 2H<sup>+</sup> → M<sup>(n+1)+</sup> – SOD + H<sub>2</sub>O<sub>2</sub> + O<sub>2</sub>; in which M = Cu (n = 1), Mn (n = 2), Fe (n = 2), Ni (n = 2)]. Among the family members, SOD1 is a copper and zinc-containing homodimer, CuZn-SOD, primarily localized in cytoplasm; SOD2 is a manganese-containing enzyme, Mn-SOD, and is exclusively localized in mitochondria; SOD3 is a copper- and zinc-containing tetramer, containing a signal peptide directing SOD3 primarily to the extracellular space (EC-SOD), and is produced by lung tissue cells (12). We investigated whether there is a functional link between miR-21 and the regulation of ROS levels through targeting a member of the SOD family, thereby, contributing to miR-21-induced tumorigenesis. In this study, we found that miR-21 changed the levels of superoxide to hydrogen peroxide in the human bronchial epithelial cells by directly targeting SOD3, and TNF $\alpha$  decreased the SOD2 levels, and these changes are linked to increased IR-induced cell transformation in miR-21-expressing cells. Our findings reveal a new mechanism to explain the role of miR-21 in promoting tumorigenesis *via* regulating cellular ROS levels.

### Materials and Methods

#### Cell lines and radiation

Immortalized human bronchial epithelial cells (NL20) were purchased from American Type Culture Collection and cultured according to the manufacturer's instructions. The cell line was verified using a soft-agar colony forming assay. Low-LET radiation was carried out using an X-ray machine (X-RAD 320, N. Branford 320 kV, 10 mA, 2-mm aluminum filtration) in our laboratory and high-LET radiation was carried out using an alternating gradient synchrotron (Fe ions, 1 GeV/amu) at Brookhaven National Laboratory. The dose rates for both high-LET IR and low-LET IR were about 1 Gy/minute.

#### Reagents

The plasmids for miR-21 expression, pCDH-CMV-MCS-EF1-copGFP (with GFP), and pCDH-CMV-MCS-EF1-Puro (without

**Authors' Affiliations:** <sup>1</sup>Departments of Radiation Oncology and <sup>2</sup>Biochemistry, Winship Cancer Institute, Emory University School of Medicine, Emory University, Atlanta, Georgia

**Note:** Supplementary data for this article are available at Cancer Research Online (<http://cancerres.aacrjournals.org/>).

**Corresponding Author:** Ya Wang, Department of Radiation Oncology, Emory University School of Medicine, 1365 Clifton Rd., Suite C5090, Atlanta, GA 30322. Phone: 404-778-1832; Fax: 404-778-1750; E-mail: ywang94@emory.edu

doi: 10.1158/0008-5472.CAN-12-0639

©2012 American Association for Cancer Research.

GFP) were purchased from SBI. The plasmid for the luciferase assay, psiCHECK-2, was purchased from Promega. The *SOD3* or *TNF $\alpha$*  encoding plasmid was purchased from GeneCopoeia. The miR-21 mimic (double strand sense mature miR-21) and miR-21 antisense inhibitor (50 nmol/L) were purchased from Thermo Fisher Scientific. The siRNA against *SOD2*, *SOD3*, *TNF $\alpha$* , the control RNA and the antibody against SOD1, SOD2, or  $\beta$ -actin was purchased from Santa Cruz Biotech Inc. The antibody against SOD3 was purchased from ENZO Life Sciences, and the antibody against TNF $\alpha$  was purchased from Cell Signaling.

### ROS detection

A total of  $0.5 \times 10^6$  cells were plated in a 60-mm dish and grown overnight at 37°C in a CO<sub>2</sub> incubator. For some transient gene-regulation experiments, the cells were transfected with the proper vector or small RNAs and incubated at 37°C for 48 hours. The cells were collected, washed with PBS, and resuspended in CM-H<sub>2</sub>DCFDA (Invitrogen, for H<sub>2</sub>O<sub>2</sub> detection) or dihydroethidium (DHE; Sigma, for O<sub>2</sub><sup>-</sup> detection) at a final concentration of 10  $\mu$ mol/L. The cells were incubated at 37°C for 30 minutes, and then kept on ice. The cells were irradiated on ice and resuspended in the medium after IR and kept at 37°C for different times; the cells were then washed with PBS and measured against the ROS level using a BD FACSCanto II flow cytometer.

### Real-time PCR

Real-time PCR was conducted as described in our previous publication (13) with the proper primers as described in Supplementary Table S1.

### Luciferase assay

A luciferase assay was conducted as described in our previous publication (13). Briefly, 293FT cells were transfected with the plasmid (psiCHECK-2) containing different 3'-UTRs from different genes with or without 100 nmol/L *hsa-miR-21* mimics in 48-well plates. The cells were harvested 48 hours after transfection, and the cells were then lysed with a luciferase assay kit (Promega) according to the manufacturer's protocol and measured on a LUMIstar Galaxy luminescent microplate reader (BMG labtechnologies).  $\beta$ -Galactosidase or *Renilla* luciferase was used for normalization.

### Cell transformation

Cell transformation was measured by using a soft-agar colony forming assay. Four percent of low melting temperature agarose and 1 $\times$  complete NL20 complete medium were mixed to obtain a 0.5% agarose concentration and then, 2 mL of 0.5% agarose–NL20 complete medium mixture was added to each well in 6-well plates and the agar was solidified at 4°C. These plates were kept in the incubator until the next day. Cells were harvested and mixed (500, 1,000, and 1,500 cells per well) with tissue culture medium containing 0.7% agar to a final agar concentration of 0.35%. Then, 2 mL of the cell suspension was immediately plated in 6-well plates coated with 2 mL of 0.5% agar in tissue culture medium per well (in triplicate), and the cells were cultured at 37°C with 5% CO<sub>2</sub>

for 3 weeks. The culture was stained with 0.2% *p*-iodonitrotrazolium violet (Sigma) or scanned for colony counting, and colonies larger than 100  $\mu$ m in diameter were counted.

### Statistical analysis

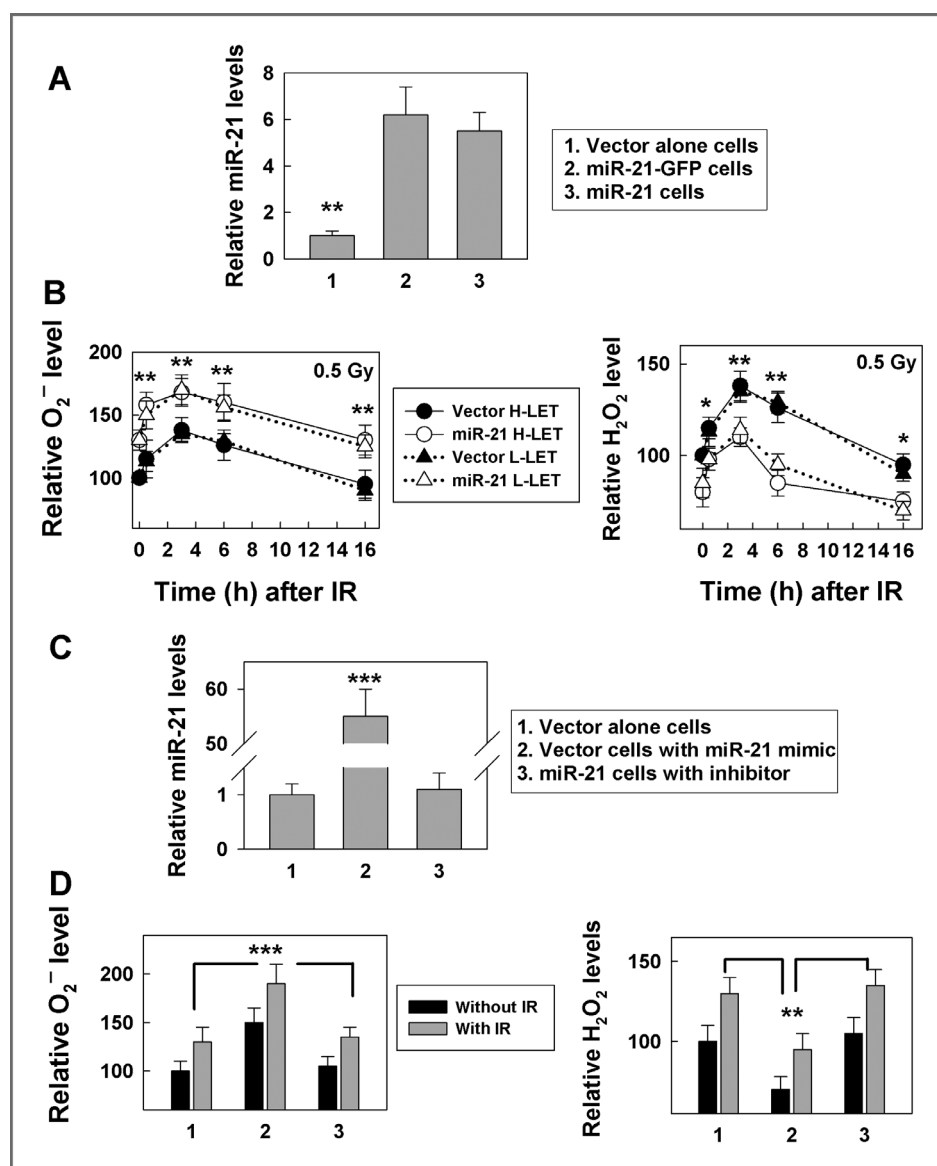
Statistical analysis of data was done using the Student *t* test. Differences with *P* < 0.05 are considered significant.

## Results

### miR-21 overexpression increases IR-induced cellular ROS levels

To establish a stable miR-21-expressing cell model, we inserted a 362 bp sequence comprising pri-miR-21 (4) into a plasmid with or without the *GFP* gene, transfected these plasmids or a vector control into the human bronchial epithelial cell line NL20, and selected for miR-21-expressing cells (Fig. 1A). The purpose of establishing 2 sets of cells overexpressing miR-21 (with or without GFP) is: (i) to confirm the relationship between miR-21 and its targets in 2 independently generated cell lines, (ii) to monitor miR-21 expression by GFP coexpression, and (iii) to detect ROS levels by flow cytometry in miR-21-expressing cells without GFP signal interference. We measured ROS (superoxide and hydrogen peroxide) levels in the cells at different times following exposure to IR [either high linear energy (LET) iron or low-LET X-rays]. The results show that miR-21 expression increased superoxide (O<sub>2</sub><sup>-</sup>) levels while reducing hydrogen peroxide (H<sub>2</sub>O<sub>2</sub>) levels (Fig. 1B, 0-hour time point). To examine whether our measurements for the superoxide or hydrogen peroxide were specific, we measured the superoxide levels in cells with polyethylene glycol (PEG)-SOD and the hydrogen peroxide levels with additional H<sub>2</sub>O<sub>2</sub>. The results showed that the (O<sub>2</sub><sup>-</sup>) levels measured by dihydroethidium (DHE) flow cytometry decreased with additional PEG-SOD (Supplementary Fig. S1A), and the (H<sub>2</sub>O<sub>2</sub>) levels measured by cellular reactive oxygen species detection assay kit (DCFDA) flow cytometry increased with additional hydrogen peroxide (Supplementary Fig. S1B). These results further supported that our measurements reflected the (O<sub>2</sub><sup>-</sup>) or (H<sub>2</sub>O<sub>2</sub>) levels. IR (0.5 Gy) stimulated the generation of superoxide and hydrogen peroxide in the cells; although, returning to nonirradiated levels at 16 hours after IR (Fig. 1B). There was no apparent difference in the ROS levels between the cells exposed to iron (high-LET) or X-ray (low-LET) IR (Fig. 1B). Furthermore, increasing the IR dose to 5 Gy did not further increase the ROS response in these cells (Supplementary Fig. S2). These results indicate that ROS generation in the cells is sensitive to IR; the ROS levels reach a maximal level at 3 hours and return to preirradiated levels within 16 hours. Although miR-21 expression increased at 3 hours after IR in the cells transfected with vector alone at this point, the miR-21 levels did not increase in cells already overexpressing miR-21 (Supplementary Fig. S3), supporting the previous observation that IR-induced miR-21 expression peaks over a short time period, (2–4). To exclude the possibility that the increased ROS level in the miR-21-overexpressing cells was because of miR-21-independent effects, we used either a miR-21 antisense inhibitor (for miR-21 overexpressing cells) or a

**Figure 1.** miR-21 overexpression changes basal and IR-induced ROS level. **A**, miR-21 levels were measured in the cells with or without stable miR-21 overexpression using a real-time PCR assay. The relative miR-21 levels are expressed as a ratio of the miR-21 level in mimic-transfected cells over the vector-transfected control cells, \*\*,  $P < 0.01$ . **B**, the ROS level [left, superoxide ( $O_2^-$ ); right, hydrogen peroxide ( $H_2O_2$ )] was measured in cells with or without stable miR-21 overexpression at the indicated time after exposure to 0.5 Gy high- or low-LET IR using a flow cytometer. The results are expressed as a percentage of the level in nonirradiated control cells and are the mean  $\pm$  SE obtained from 2 separate experiments. \*,  $P < 0.05$ ; \*\*,  $P < 0.01$ . **C**, miR-21 levels were measured using the cells transfected with the miR-21 mimic, inhibitor, or control RNA (50 nmol/L) at 48 hours after transfection with a real-time PCR assay. \*\*\*,  $P < 0.001$ . **D**, the ROS level (left,  $O_2^-$ ; right,  $H_2O_2$ ) was measured at 3 hours after exposure of the cells (at 48 hours after transfection with miR-21 mimic, inhibitor, or control RNA) to 0.5 Gy low-LET IR by flow cytometry as described in Materials and Methods. Numbers 1, 2, and 3 reflect the data from the same cells as described in C. The data are the mean  $\pm$  SE and obtained from 3 separated experiments; \*\*,  $P < 0.01$ ; \*\*\*,  $P < 0.001$ .



miR-21 mimic (for control cells) and measured the ROS levels. The results show that after miR-21 was upregulated in these cells (Fig. 1C); the ROS levels changed and IR enhanced this phenotype (Fig. 1D). In contrast, the miR-21 inhibitor abrogated the miR-21-induced ROS changes (Fig. 1D). These results confirm that miR-21 increases the basal and IR-induced superoxide level in the cells. The higher superoxide level and lower hydrogen peroxide level in the miR-21-overexpressing cells suggest that miR-21 might be targeting *SODs*.

### miR-21 directly targets *SOD3*

To address whether miR-21 targets *SODs*, we measured the levels of *SOD1*, *SOD2*, and *SOD3* in cells with or without miR-21 overexpression at different times following IR exposure. The results show that nonirradiated cells overexpressing miR-21 have unchanged *SOD1* levels but *SOD2* and *SOD3* levels were reduced (Fig. 2A). IR (0.5 Gy) induced a transient increase in

*SOD1* and *SOD2* expression in control cells, whereas miR-21 overexpression dramatically reduced this effect (Fig. 2A). Cells exposed to a higher dose (5 Gy) did not respond differently (Supplementary Fig. S4). The lower levels of *SOD2*/*SOD3* in the miR-21-overexpressing cells suggest that miR-21 might target *SOD2* and *SOD3*. To test this hypothesis, we conducted a matching search by using PicTar, TargetScan3.1, MiRanda, and miRGen tools and identified one potential miR-21 binding site in the 3'-UTR of *SOD3* (Fig. 2B, Supplementary Fig. S5). To show that miR-21 targets *SOD3* directly, the *SOD3* complementary site was cloned into the 3'-UTR of the firefly luciferase gene and cotransfected with miR-21 in 293FT cells. The results showed that the miR-21 binding site resulted in a substantial inhibition of luciferase activity. This inhibitory effect was lost when the binding site was deleted (Fig. 2B), indicating that the site in the 3'-UTR of *SOD3* represents an authentic miR-21 binding site and confirming that *SOD3* is a direct target of

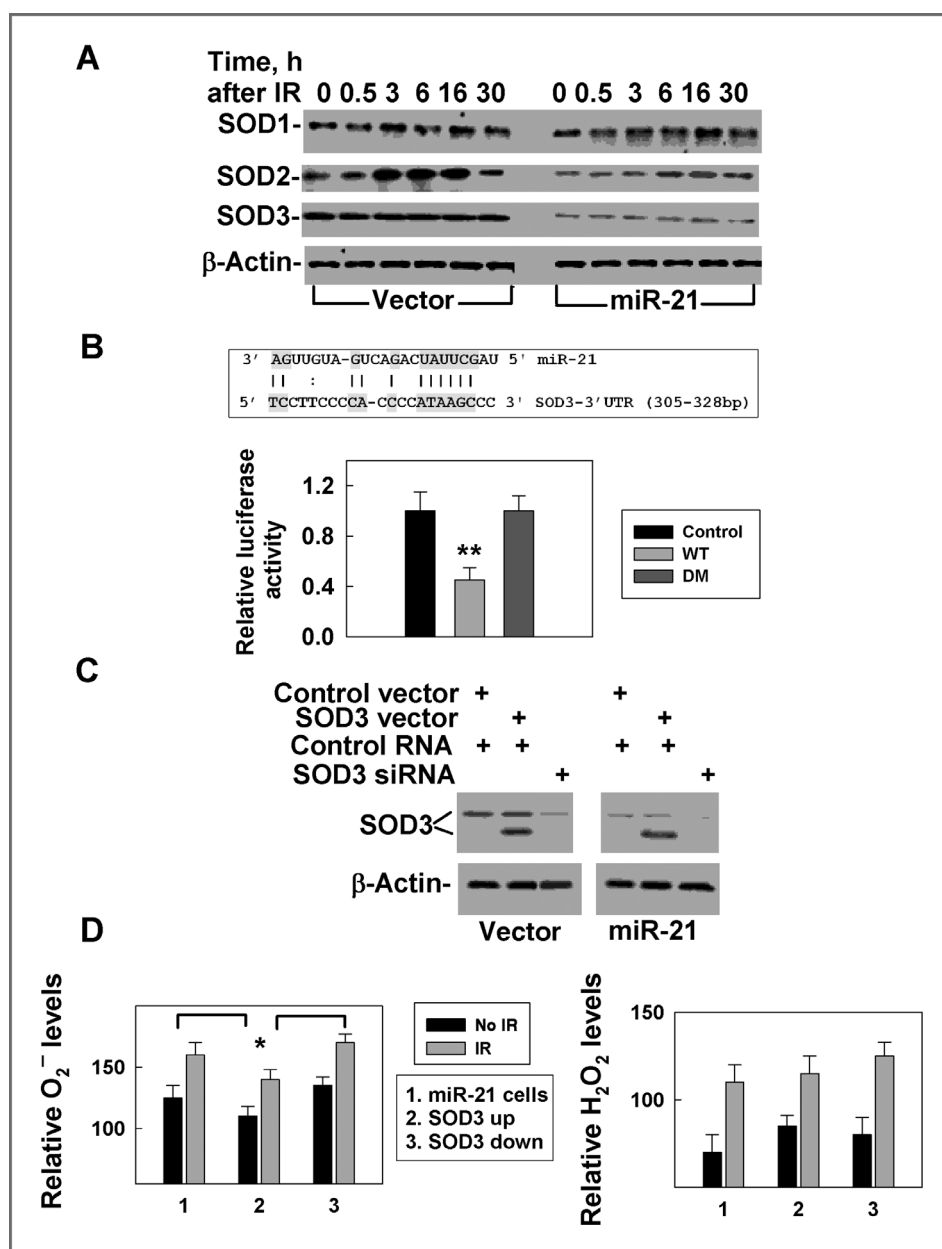


**Figure 2.** miR-21 directly targets *SOD3*. **A**, SOD levels were measured in cells with or without stable miR-21 overexpression at different times after 0.5 Gy low- or high-LET IR by Western blot analysis. β-Actin was used as an internal loading control. **B**, potential miR-21 binding site in the 3'-UTR of *SOD3* and the effects of the binding site on luciferase activity. 293T cells were transfected with a firefly luciferase reporter plasmid containing a partial 3'-UTR of *SOD3* with the putative miR-21 binding site (WT) or without the binding site or deleted mutation (DM). Luciferase activity was assayed 48 hours after transfection with miR-21 mimic (miR-21) or control RNA (mock) and are standardized by β-galactosidase activity. \*\*,  $P < 0.01$ . **C**, SOD3 levels were measured in cells with up- or downregulation of SOD3 expression in cells overexpressing miR-21 or a vector by Western blot analysis. β-Actin was used as an internal loading control. **D**, ROS levels (left, O<sub>2</sub><sup>-</sup>; right, H<sub>2</sub>O<sub>2</sub>) were measured in cells with up- or downregulation of SOD3 at 3 hours after 0.5 Gy low-LET ionizing radiation. The data are an average of three separate experiments. \*:  $P < 0.05$ .

miR-21. To examine whether miR-21 affected ROS through targeting *SOD3*, we upregulated *SOD3* expression by transfecting a cDNA without 3'-UTR region in cells overexpressing miR-21 and compared them with cells with reduced levels of *SOD3* expression by siRNA. Transfection of the *SOD3* cDNA generated a non-glycosylated form (30 kD) of *SOD3* (14) that is recognized by the *SOD3* antibody (Fig. 2C). This non-glycosylated form of *SOD3* seems to be active because overexpressing it upregulated *SOD3* activity (Supplementary Fig. S6), and IR increased ROS levels in cells ectopically expressing *SOD3* (Fig. 2D). Conversely, reducing the endogenous *SOD3* levels by siRNA (Fig. 2C) was sufficient to change the basal- and IR-induced ROS levels (Fig. 2D). These results support a model in which miR-21 overexpression results in an ROS change in

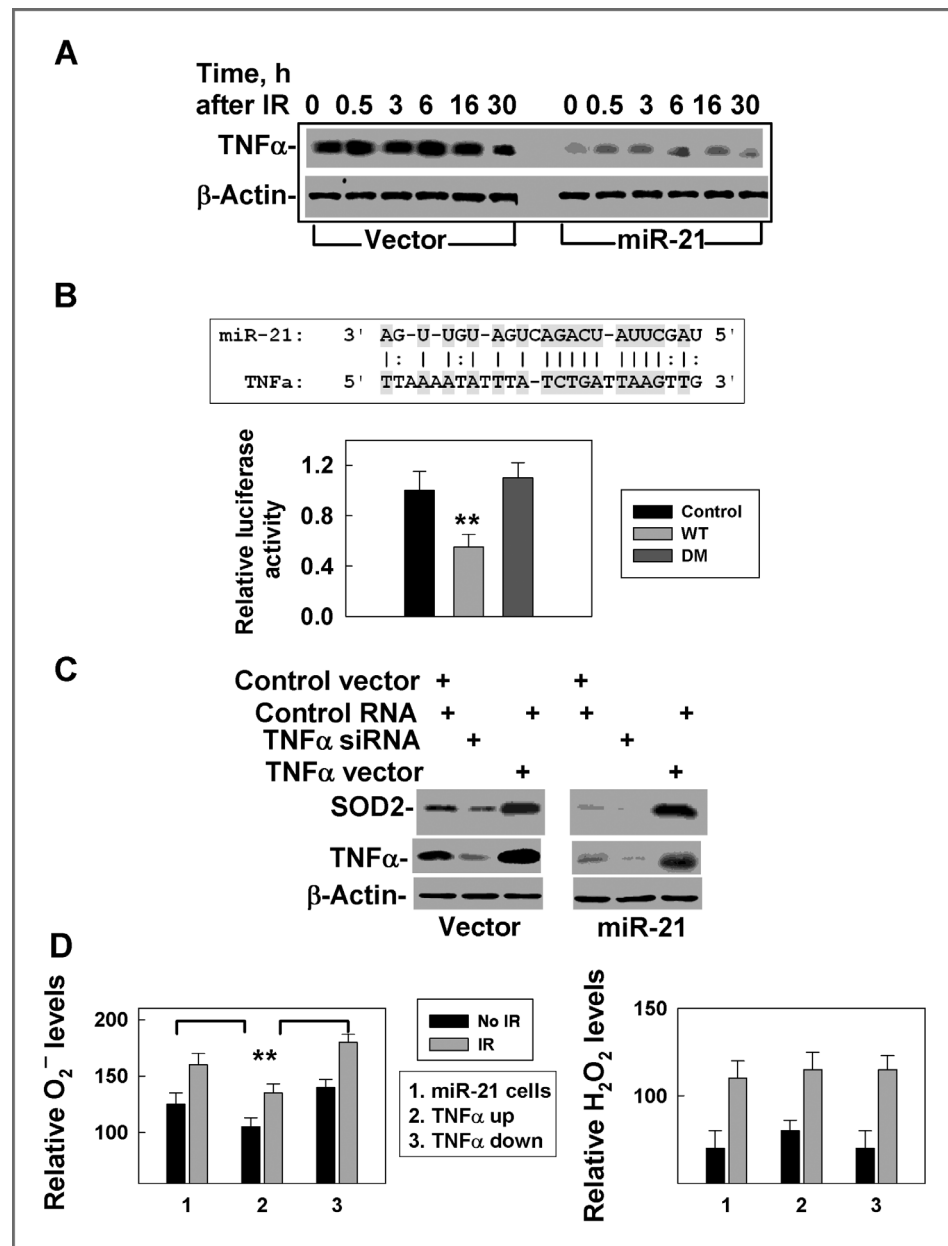
the irradiated cells by targeting *SOD3*. *SOD3* is an extracellular enzyme, and it has been established that the extracellular environment also plays an important role in influencing genomic integrity (15). Thus, *SOD3* may contribute to protecting cells from ROS-induced genetic instability.

#### miR-21 directly targets *TNFα* and influences *SOD2* levels

Reduced *SOD2* protein levels following miR-21 overexpression has been previously reported by another group (16), but the mechanism leading to this phenotype is unknown, as there was no predictable miR-21 binding site in 3'-UTR of *SOD2*. Next, we sought the candidates that could upregulate *SOD2* expression and be targeted by miR-21. *TNFα* came to light because it can induce *SOD2* expression (17, 18), and the level



**Figure 3.** miR-21 directly targets *TNF $\alpha$* , an SOD2 inducer. **A**, *TNF $\alpha$*  levels were measured by Western blot analysis in cells with or without stable miR-21 overexpression at different times after 0.5 Gy low-LET ionizing radiation.  $\beta$ -Actin was used as an internal loading control. **B**, potential miR-21 binding site in the 3'-UTR of *TNF $\alpha$*  and the effects of the binding site on the luciferase activity. Luciferase activity was assayed 48 hours after transfection with the miR-21 mimic (miR-21) or control RNA (mock). \*\*,  $P < 0.01$ . **C**, effects of *TNF $\alpha$*  on SOD2 expression. Cells overexpressing miR-21 or vector-transfected cells were transiently transfected with the *TNF $\alpha$*  cDNA (without 3'-UTR) or siRNA. At 48 hours after transfection, the cells were collected and analyzed by Western blot analysis.  $\beta$ -Actin was used as an internal loading control. **D**, ROS levels (left,  $O_2^-$ ; right,  $H_2O_2$ ) were measured using the cells (as described in C), with up- or downregulated *TNF $\alpha$*  at 3 hours after 0.5 Gy low-LET IR. The data are an average of 3 separate experiments. \*\*,  $P < 0.01$ .



of *TNF $\alpha$*  expression decreased in miR-21-overexpressing cells compared with vector-transfected control cells (Fig. 3A). IR increased the levels of *TNF $\alpha$* , whereas miR-21 overexpression dramatically reduced both the basal and the IR-induced increase (Fig. 3A). In addition, the low *TNF $\alpha$*  levels in 5 Gy irradiated cells (Supplementary Fig. S4) further support the concept that *TNF $\alpha$*  might be a target of miR-21. In addition, the 3'-UTR of *TNF $\alpha$*  contains a potential miR-21 binding site (Fig 3B, Supplementary Fig. S7). To verify that *TNF $\alpha$*  is a miR-21 target, we tested luciferase activity driven by the 3'-UTR region of *TNF $\alpha$* . These results indicate that *TNF $\alpha$*  is a target of miR-21 (Fig. 3B). Our results also confirm that *TNF $\alpha$*  stimulates transcription of SOD2 (18). In addition, upregulating *TNF $\alpha$*  (without 3'-UTR) in cells overexpressing miR-21 or downre-

gulating *TNF $\alpha$*  by using siRNA in vector-transfected control cells (Fig. 3C), altered *SOD2* mRNA levels (Supplementary Fig. S8) and *TNF $\alpha$*  protein levels (Fig. 3C), as well as the SOD2 activities (Supplementary Fig. S9). More importantly, such changes in *TNF $\alpha$*  expression affected basal- and IR-induced increases in ROS (Fig. 3D). Because there were no apparent differences in the levels and activities of catalase or glutathione peroxidases between miR-21-upregulated cells and their counterpart control cells (Supplementary Fig. S10), these results exclude the possibility that miR-21 affects the ROS level through other pathways. These results strongly support the conclusion that the IR-induced increase in superoxide levels in miR-21-overexpressing cells is at least due, in part, to miR-21 targeting of *TNF $\alpha$* , thereby decreasing SOD2 levels.

### miR-21 increases IR-induced cell transformation via targeting *SOD3* and *TNF $\alpha$*

It is known that increased levels of intracellular ROS induce a cellular genotoxic stress response (19) and promote cellular transformation (10). Previously, we reported that overexpressing miR-21 can result in a conversion of nontumorigenic human cells to tumorigenic cells and that exposure to IR enhanced this conversion (4). We also showed in this study that hydrogen peroxide levels decreased but superoxide levels increased in the miR-21-overexpressing cells. Since superoxide has been shown to be a more powerful factor than hydrogen peroxide at stimulating cell proliferation (20), it is possible that miR-21-induced tumorigenesis (2, 4) is partially due to the high superoxide level generated in the cells. To test this hypothesis, we used cell-colony forming in soft agar to examine the effects of miR-21 on IR-induced transformation. We compared the cell transformation among the cells with or without miR-21 overexpression and with or without *SOD3* or *TNF $\alpha$*  upregulation in the miR-21-overexpressing cells, following 4 months exposure to a low dose (0.5 Gy) of X-ray exposure. The results showed that nonirradiated cells lacking miR-21 overexpression generated very few colonies, whereas cells overexpressing miR-21 displayed significant colony formation (Fig. 4A). Following IR exposure, both cell lines generated elevated numbers of colonies as compared with nonirradiated cells. Furthermore, the miR-21-overexpressing cells displayed elevated colony formation as compared with cells transfected with vector alone (Fig. 4A). These results suggest that miR-21 promotes IR-induced cell transformation.

To examine whether the miR-21-increased IR-induced cell transformation was linked to miR-21-increased superoxide, we irradiated cells overexpressed with miR-21 and upregulated *SOD3* or *TNF $\alpha$*  expression, and compared soft-agar colony formation among the cells after 4 months of subcultures. Increased expression of *SOD3* or *TNF $\alpha$*  at the time of radiation decreased the number of IR-induced soft-agar colonies in the miR-21-overexpressing cells (Fig. 4B), suggesting that miR-21-stimulated cell transformation is linked to miR-21-increased superoxide. Because miR-21 plays an important role in initiating and promoting tumorigenesis (2–4), our results indicate that a component of miR-21-stimulated cell transformation occurs by increasing superoxide and may be associated with its role in tumor development (Fig. 4C).

### Discussion

In this study, we reported for the first time that miR-21 affects ROS levels through targeting *SOD3* and *TNF $\alpha$*  (indirectly affecting *SOD2*), which might be linked to the role of miR-21 in carcinogenesis. Although IR stimulated an increase in the ROS levels in the cells, we did not observe the IR dose–response effects: 5 Gy irradiated cells did not show a dramatic change in ROS levels than 0.5 Gy irradiated cells. In addition, we did not find any dramatic difference in ROS levels between high-LET and low-LET irradiated cells. These phenotypes might be due to the fact that the amount of ROS generation per cell is relatively consistent, which does not change with a radiation dose increase or quality change (21, 22). As mentioned in these

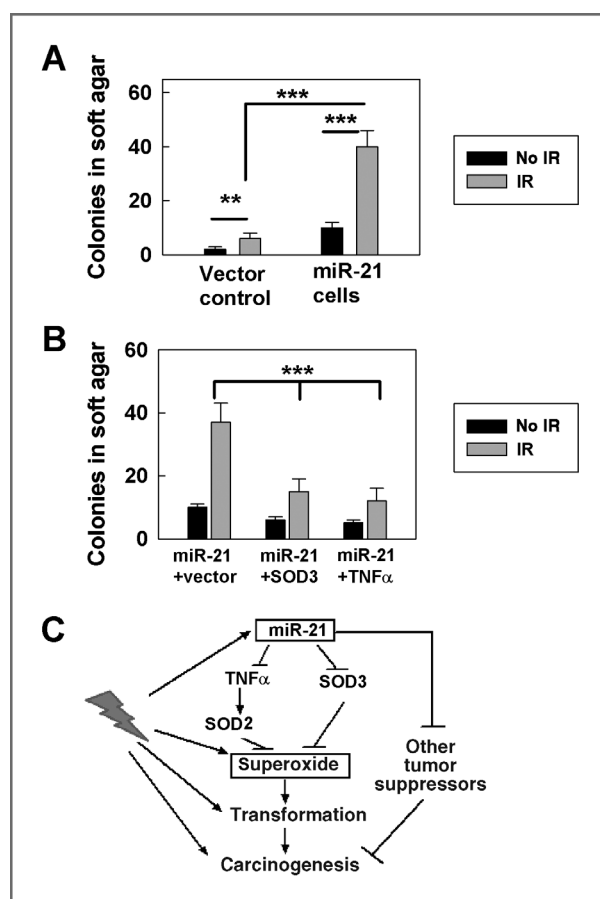


**Figure 4.** miR-21 increases IR-induced cell transformation partially via targeting *SOD3* and *TNF $\alpha$* . A, the data reflect the number of colonies that were grown from cells with or without miR-21 overexpression in soft agar for 3 weeks. The results were obtained from 2 separate experiments with triple dishes per sample in each experiment. \*\*,  $P < 0.01$ ; \*\*\*,  $P < 0.001$ . B, similar experiments were carried out as described in A, but with the cells upregulated either by *SOD3* or *TNF $\alpha$*  cDNAs. The results were confirmed in 2 separate experiments with triple dishes per sample in each experiment. \*\*\*,  $P < 0.001$ . C, a model proposed to explain how miR-21 could stimulate cell transformation partially through increasing superoxide, thereby contributing to the role of miR-21 in carcinogenesis. miR-21-increased IR-induced superoxide levels through targeting *SOD3* and *TNF $\alpha$*  (a transcriptional activator of *SOD2*), which contributes to IR-induced cell transformation and carcinogenesis.

articles, their results are consistent with a threshold of an all-or-nothing response (21, 22). After 0.5 Gy exposure, we observed a clear change in ROS, indicating that such a dose is enough to initiate the change in the ROS levels; although at 24 hours after IR, the ROS level reverted back to the levels similar to that in nonirradiated cells, and we believe that the transient change would induce some consequences that affect the cell biologic functions. Of course, these predictions need future experiments to elucidate.

The difference in the ROS levels between miR-21-upregulated cells and their control counterparts are consistent, which provides additional evidence that the change in ROS might contribute to the role of miR-21 in carcinogenesis. Carcinogenesis is a complicated process and involves more

proteins and pathways. Upregulating miR-21 could result in nontumorigenic human cells becoming tumorigenic (4) or mouse lymphomas (2), confirming the tumorigenesis of miR-21. The role of miR-21 in carcinogenesis is believed to be linked to multiple targets of miR-21, such as *PTEN*, *PDCD4*, and *TPMI* (5–9); however, the whole picture for miR-21-induced tumorigenesis remains unclear. We previously reported that radiation enhanced the role of miR-21 in tumorigenesis (4) and the transformation results in this study also support it. However, how radiation enhances the miR-21's tumorigenesis needs more studies. Our results, shown in this study, strongly support that the effects of miR-21 on the ROS level cooperate with the effects of other miR-21 targets and contribute to miR-21's carcinogenesis.

#### Disclosure of Potential Conflict of Interest

No potential conflicts of interest were disclosed.

#### Authors' Contributions

**Conception and design:** X. Zhang, H. Wang, Y. Wang

**Development of methodology:** X. Zhang, W.-L. Ng, E. Werner, Y. Wang

**Acquisition of data (provided animals, acquired and managed patients, provided facilities, etc.):** X. Zhang, L. Tian, Y. Wang

**Analysis and interpretation of data (e.g., statistical analysis, biostatistics, computational analysis):** X. Zhang, P. Doetsch, Y. Wang

**Writing, review, and/or revision of the manuscript:** E. Werner, P. Doetsch, Y. Wang

**Administrative, technical, or material support (i.e., reporting or organizing data, constructing databases):** X. Zhang, P. Wang, Y. Wang

**Study supervision:** X. Zhang, Y. Wang

#### Acknowledgments

The authors thank the support team at Brookhaven National Laboratory for helping with the high-LET IR, members of the Wang laboratory for helpful discussion, and Doreen Theune for editing the manuscript.

#### Grant Support

This work is supported by grants from NIH (GM080771) and NASA (NNX11AC30G) to Y. Wang.

The costs of publication of this article were defrayed in part by the payment of page charges. This article must therefore be hereby marked *advertisement* in accordance with 18 U.S.C. Section 1734 solely to indicate this fact.

Received February 20, 2012; revised June 20, 2012; accepted July 16, 2012; published OnlineFirst July 25, 2012.

#### References

- Croce CM. miRNAs in the spotlight: understanding cancer gene dependency. *Nat Med* 2011;17:935–6.
- Medina PP, Nolde M, Slack FJ. OncomiR addiction in an *in vivo* model of microRNA-21-induced pre-B-cell lymphoma. *Nature* 2010;467:86–90.
- Hatley ME, Patrick DM, Garcia MR, Richardson JA, Bassel-Duby R, van Rooij E, et al. Modulation of K-Ras-dependent lung tumorigenesis by microRNA-21. *Cancer Cell* 2010;18:282–93.
- Zhu Y, Yu X, Fu H, Wang H, Wang P, Zheng X, et al. MicroRNA-21 involves radiation-promoted liver carcinogenesis. *Int J Clin Exp Med* 2010;3:211–22.
- Asangani IA, Rasheed SAK, Nikolova DA, Leupold JH, Colburn NH, Post S, et al. MicroRNA-21 (miR-21) post-transcriptionally downregulates tumor suppressor Pdc4d and stimulates invasion, intravasation and metastasis in colorectal cancer. *Oncogene* 2007;27:2128–36.
- Zhu S, Wu H, Wu F, Nie D, Sheng S, Mo Y-Y. MicroRNA-21 targets tumor suppressor genes in invasion and metastasis. *Cell Res* 2008;18:350–9.
- Lu Z, Liu M, Stribinskis V, Klinge C, Ramos K, Colburn N. MicroRNA-21 promotes cell transformation by targeting the programmed cell death 4 gene. *Oncogene* 2008;27:4373–9.
- Papagiannakopoulos T, Shapiro A, Kosik KS. MicroRNA-21 targets a network of key tumor-suppressive pathways in glioblastoma cells. *Cancer Res* 2008;68:8164–72.
- Seike M, Goto A, Okano T, Bowman ED, Schetter AJ, Horikawa I, et al. MiR-21 is an EGFR-regulated anti-apoptotic factor in lung cancer in never-smokers. *Proc Natl Acad Sci U S A* 2009;106:12085–90.
- Behrend L, Henderson G, Zwacka RM. Reactive oxygen species in oncogenic transformation. *Biochem Soc Trans* 2003;31:1441–4.
- Cao J, Schulte J, Knight A, Leslie NR, Zagodzko A, Bronson R, et al. Prdx1 inhibits tumorigenesis *via* regulating PTEN/AKT activity. *EMBO J* 2009;28:1505–17.
- Zelko IN, Mariani TJ, Foltz RJ. Superoxide dismutase multigene family: a comparison of the CuZn-SOD (SOD1), Mn-SOD (SOD2), and EC-SOD (SOD3) gene structures, evolution, and expression. *Free Radic Biol Med* 2002;33:337–49.
- Yan D, Ng W, Zhang X, Wang P, Zhang Z, Mo Y, et al. Targeting DNA-PK and ATM with miR-101 sensitizes tumors to radiation. *PLoS ONE* 2010;5:e11397.
- Marklund S. Human copper-containing superoxide dismutase of high molecular weight. *Proc Natl Acad Sci U S A* 1982;79:7634–8.
- Nguyen David H, Oketch-Rabah Hellen A, Illa-Bochaca I, Geyer Felipe C, Reis-Filho Jorge S, Mao J-H, et al. Radiation acts on the microenvironment to affect breast carcinogenesis by distinct mechanisms that decrease cancer latency and affect tumor type. *Cancer Cell* 2011;19:640–51.
- Fleissner F, Jazbutyte V, Fiedler J, Gupta SK, Yin X, Xu Q, et al. Short communication: asymmetric dimethylarginine impairs angiogenic progenitor cell function in patients with coronary artery disease through a microRNA-21-dependent mechanism. *Circ Res* 2010;107:138–43.
- Wispe JR, Clark JC, Warner BB, Fajardo D, Hull WE, Holtzman RB, et al. Tumor necrosis factor- $\alpha$  inhibits expression of pulmonary surfactant protein. *J Clin Invest* 1990;86:1954–60.
- Xu Y, Kiningham KK, Devalaraja MN, Yeh C-C, Majima H, Kasarskis EJ, et al. An intronic NF- $\kappa$ B element is essential for induction of the human manganese superoxide dismutase gene by tumor necrosis factor- $\alpha$  and interleukin-1 $\beta$ . *DNA Cell Biol* 1999;18:709–22.
- Rowe L, Degtyareva N, Doetsch P. DNA damage-induced reactive oxygen species (ROS) stress response in *Saccharomyces cerevisiae*. *Free Radic Biol Med* 2008;45:1167–77.
- Burdon RH. Superoxide and hydrogen peroxide in relation to mammalian cell proliferation. *Free Radic Biol Med* 1995;18:775–94.
- Leach JK, Van Tuyle G, Lin P-S, Schmidt-Ullrich R, Mikkelsen RB. Ionizing radiation-induced, mitochondria-dependent generation of reactive oxygen/nitrogen. *Cancer Res* 2001;61:3894–901.
- Mikkelsen RB, Wardman P. Biological chemistry of reactive oxygen and nitrogen and radiation-induced signal transduction mechanisms. *Oncogene* 2003;22:5734–54.